A COMPREHENSIVE NUMERICAL STUDY OF ENERGY EFFICIENCY ANALYSIS OF A DOUBLE PIPE GAS COOLER BASED ON SECOND LAW ANALYSIS

by

Dazhang YANG [a], ***Naixin WANG*** [b], ***Jing XIE*** [c*], **and** ***Jinfeng WANG*** [d]

[a] College of Food Science and Technology, Shanghai Ocean University, Shangai, China
[b] Shanghai Professional Technology Service Platform on Cold Chain Equipment Performance and Energy Saving Testing Evaluation, Shangai, China
[c] Shanghai Engineering Research Center of Aquatic Product Processing and Preservation, Shangai, China
[d] National Experimental Teaching Demonstration Center for Food Science and Engineering, Shanghai Ocean University, Shangai, China

Original scientific paper
https://doi.org/10.2298/TSCI210719052Y

A numerical simulation of energy efficiency in commercially available double pipe heat exchangers in the market was investigated based on the Second law of thermodynamics in this paper. The effects of CO_2 mass-flow rate, water mass-flow rate, pressure, CO_2 inlet temperature, and water inlet temperature of the double pipe heat exchanger were considered to evaluate the energy efficiency by analyzing entropy generation, exergy destruction, and entransy dissipation. The changes of the entropy generation, the changes of exergy destruction, and entransy dissipation are similar regardless of the operating conditions. Pressure has the most significant effect on the energy efficiency of the double pipe gas cooler compared to other operating conditions but negligible on the exergy destruction. The pressure, flow rate, and inlet temperature have completely different effects on energy efficiency depending on the region. The entropy generation and entransy dissipation at $y = 0$ m to $y = 0.05$ m (y-axis is the radial direction) decrease with increasing pressure and the opposite after that. The increase of CO_2 inlet temperature at $y < 0.5$ m is accompanied by an increase of entropy generation, exergy destruction, and entransy dissipation but this situation disappears after $y = 0.5$ m. Entropy generation, exergy destruction, and CO_2 and water mass-flow rate are first negatively and then positively correlated with the cut-off point at $y = 0.1$ m.

Key words: entropy generation, exergy destruction, entransy dissipation, supercritical CO_2

Introduction

The use of chlorofluorocarbons (CFC) as refrigerants in refrigeration systems causes environmental degradation including global warming, ozone depletion, and air pollution due to GHG emissions, which has led international organizations to rush to find natural refrigerants to replace them. The advent of the Montreal Protocol [1] led countries to agree to find new non-polluting refrigerants to replace CFC and hydrofluorocarbons at the end of the 20th century. A look back at the numerous studies on the properties of CO_2 [2-6] conducted in the last decade shows that CO_2 is one of the most highly regarded natural refrigerants attributing to the fact

* Corresponding author, e-mail: jxie@shou.edu.cn

that it is non-flammable, non-toxic, easily available, and cheap. In the aforementioned literature, both Elbarghthi *et al.* [7] and Zhang *et al*. [3] have used numerical simulation research to demonstrate that the buoyancy caused by the different structure of the heat exchange tube has a great influence on the heat transfer coefficient [HTC]. Zhang *et al*. [4], on the other hand, experimented with vertical heating tubes over a wide range of mass-flow rates, and a large amount of experimental data led him to a new correlation equation. Joneydi *et al*. [5] and Wang *et al*. [6] are investigating trans-critical CO_2 systems with the aim of obtaining high COP and reducing costs. More importantly, CO_2 as a refrigerant has a high volume cooling capacity and good heat transfer performance [8]. Several heat transfer studies have been done in single tubes [7, 9-12] mainly exploring the secrets of complex flow heat transfer properties of CO_2, where keeping wall temperature and heat flux constant are required as boundary conditions. Elbarghthi *et al*. [7] and Yang *et al*. [10] both studied how to suppress the deterioration of supercritical CO_2 heat transfer in a vertical heating tube at constant heat flux and temperature, with the difference that yang studies a spiral tube, while Liu *et al*. [9] studied how to enhance CO_2 heat transfer in a horizontal tube at a non-uniform heat flux. Luo *et al*. [12] reviewed and summarizes the heat transfer characteristics of CO_2 in a vertical heating tube.

Most research on heat exchangers has focused partly on automotive air conditioning [13-15] limited by the higher air temperature of secondary flow [16] and partly on printed circuit heat exchangers [17-20] limited by the high cost. Ameur *et al.* [21] compared the effect of circular and elliptical perforated baffles on plate heat exchanger performance and concluded that elliptical was superior to circular. Menni *et al.* [22] tried to add vortex generators in the channels to improve heat exchanger performance. Karima *et al.* [23] designed a new butterfly baffle geometry configuration improve tubular heat exchanger performance. Han *et al.* [24] presented a review of the micro-channel heat exchanger development applied in an air-conditioning system. He pointed out the importance of accurately predicting pressure losses and heat transfer characteristics before designing micro-channel heat exchangers. The steep increase and decrease in specific heat and the sudden drop in density cause the heat transfer characteristic of CO_2 to be completely different from those of other constant masses. Therefore, a large number of investigations have mainly explored the secrets of complex flow heat transfer properties of CO_2.

Liu *et al.* [2, 9] studied the heat transfer characteristics of supercritical CO_2 in tubes with different structures. In the vertical tube, HTC gradually increases first, then decreases rapidly, and peaks at the pseudo-critical point. However, in the horizontally oriented HC tube, The buoyancy effect causes a violent oscillation process in HTC, which indicates a weak heat transfer stability. As the inclination angle decreases in the vertical spiral tube, the unevenness of the circumferential HTC becomes more obvious. Jiang *et al.* [25-27] have done extensive research on the supercritical CO_2 heat transfer characteristics in vertical tubes. They pointed out that the heat flux is always positively correlated with the HTC, but then the upward and downward flowing HTC move in the opposite direction when the heat flux continues to increase. Xu *et al.* [28] experimentally compared the heat transfer in a small serpentine vertical tube and a straight tube. They concluded that the reason why the serpentine tube has better heat transfer performance than the straight tube is that the secondary flow due to the centrifugal force of the serpentine tube enhanced the heat transfer. Zhang *et al.* [29] conducted a numerical simulation investigation on the heat transfer characteristics of supercritical CO_2 in horizontal semicircular micro-tubes. It was found that specific heat would be in occupying more percentage in influencing the heat transfer process with an absence of buoyancy. Lei *et al.* [30] did experiments in order to study the heat exchange situation of supercritical CO_2 in a small vertical tube, especially in the case of low mass flux and high heat flux. They found that the buoyancy force in the small channel plays a decisive role in heat transfer under such conditions.

Despite the concept of exergy is of great important and the wide application of CO_2 refrigeration cycles which is considered an efficient and environment-friendly system attributed to the complex properties of CO_2 near the critical point widely used in automotive air conditioning, food refrigeration, and heat pumps [14]. Cao *et al.* [31] established a theoretical model to compare the heating performance with internal heat exchanger (IHX) and with an absence of IHX. The inlet water temperature of the IHX is the main factor affecting the COP. The presence of IHX at higher temperatures such as 313.15 K helps to improve the COP. Considering comprehensively, he suggested that the length of the heat exchanger should not exceed 2.5 m. Cao *et al.* [32] did an energy analysis with a trans-critical CO_2 heat pump. It is the fact that the presence of IHX worsens the optimal discharge pressure. Reducing the ambient temperature and increasing the inlet and outlet water temperatures also can achieve that. The presence of IHX increases the COP by 6.65% and reduces the total power consumption by 6.22%. Fang *et al.* [33] analyzes the optimal discharge pressure and cycling state parameters with various IHX efficiencies. The irreversibility and cycling of the main components are discussed from an entropy point of view, and the use of IHX increases the COP of CO_2 systems by 14.5-18.5%.

There is little energy analysis of heat exchangers with specific structures. Hashemian *et al.* [34] made a numerical study to design the optimal conical casing heat exchanger structure. The entropy generation, entropy generation number, heat exchanger reversibility norm, heat transfer improvement number, and effectiveness-NTU were selected as the main parameters for the energy analysis, and the most suitable geometry was selected, where the efficiency and heat transfer improvement number increased by 55% and 40%, respectively. Hamed *et al.* [1] found in experimental studies that exergy destruction is positively correlated with mass-flow rate, inlet temperature, and coil diameter. The largest increase in fire losses occurs in parallel flow configurations. Coil spacing has almost no effect on exergy destruction. The curve direction of the dimensionless exergy destruction, e, differs from that of the exergy destruction, E. The lower the inlet temperature, the higher the hot water flow rate, and the higher the inlet temperature, the lower the cold water flow rate, which can increase the second law efficiency of the heat exchanger. Jafarzad *et al.* [35] proposed a combined approach applied on the annular side to experimentally study the energy efficiency including the exergy and energy of a vertical double tube heat exchanger. It was shown to indeed improve the performance with that method.

A numerical simulation of energy efficiency in commercially available double pipe heat exchangers in the market was investigated based on the Second law of thermodynamics in this paper. The effects of CO_2 mass-flow rate, water mass-flow rate, pressure, CO_2 inlet temperature, and water inlet temperature of the double pipe heat exchanger were considered to evaluate the energy efficiency by analyzing entropy generation, exergy destruction, and entransy dissipation.

Numerical simulation

Numerical model

The structure of the double pipe gas cooler was shown in fig. 1 and mesh in fig. 2. The available product in the market consists of three sections in parallel, and one of them is taken as the simulated object to save simulation time. The main dimensions of the double pipe gas cooler are shown in tab. 1. The CO_2 inlet is at $x = 0.1775$ m and the outlet is at $x = –0.1775$ m. Due to the special nature of the double pipe heat exchanger tube as a waist-shaped tube, ten straight sections of the tube are taken as a reference to study the variation of its parameters along the y-axis, including the straight sections of the double pipe gas cooler inlet and outlet. The CO_2 flows through the shell side of the double pipe gas cooler, and water flows through the tube side, counter-current heat transfer is adopted in the heat exchange process.

Table 1. The main dimensions of the double pipe gas cooler

Dimension	
Gas cooler length	495 mm
Gas cooler width	534.87 mm
Gas cooler height	168 mm
Inner tube diameter	19 mm
Outer tube diameter	28 mm
Tube wall thickness	1.5 mm

Following assumptions were required in the simulation:

– uniform flow on the tube side,
– uniform flow at the shell side inlet,
– heat conduction exists only in the vertical direction of the tube wall,
– ideal counter-flow between CO_2 and water, and
– the double pipe heat exchangers are placed horizontally.

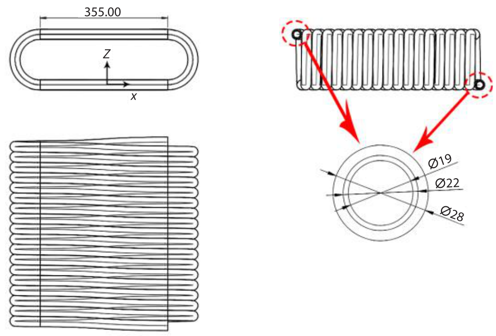

Figure 1. Numerical model

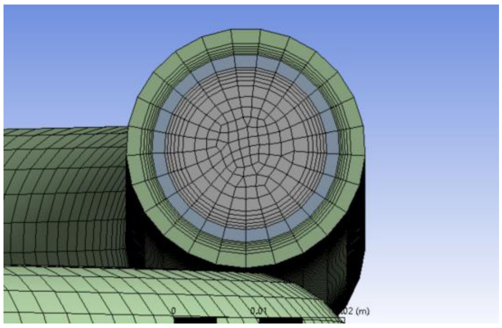

Figure 2. Grid partition

The global heat transfer processes were simulated using ANSYS FLUENT 19.0. SST k-ω turbulent model [36-39] was selected in this paper. The NIST refprop 9.11 was used to reference the properties. Mass-flow inlet and pressure-outlet [40-45] were chosen as the boundary conditions. Table 2 shows the details of the simulated working conditions. Pressure-velocity coupling and SIMPLE scheme were selected. As for the residuals, there are all 10^{-3} except for the energy which is 10^{-6}.

Table 2. The initial data for the simulations

$\dot{m}_w$ [kgs^{-1}]	$\dot{m}_r$ [kgs^{-1}]	$T_{r,in}$ [K]	$T_{w,in}$ [K]	P [MPa]
0.6	0.19	293.15	343.15	7.5
0.7	0.23	295.15	353.15	8
0.8	0.27	297.15	363.15	8.5
0.9	0.31	299.15	373.15	9
1.0	0.35	301.15	378.15	10
1.1	0.39	303.15	383.15	11
1.2	0.58	305.15	388.15	12

Governing equations

A steady-state method was used in the simulation. The equation for conservation of mass, or continuity equation:

$$\frac{\partial\left(\rho u_j\right)}{\partial x_j}=0 \tag{1}$$

Conservation of momentum is described:

$$\frac{\partial}{\partial x_j}\left(\rho u_i u_j\right)=\frac{\partial}{\partial x_j}\left[\mu_{\text{eff}}\left(\frac{\partial u_i}{\partial x_j}+\frac{\partial u_j}{\partial x_i}\right)-\frac{2}{3}\mu_{\text{eff}}\frac{\partial u_k}{\partial x_k}\right]-\frac{\partial p}{\partial x_j}+\rho g_i \tag{2}$$

where μ_{eff} is the effective viscosity which is calculated:

$$\mu_{\text{eff}}=\mu+\mu_{\text{t}} \tag{3}$$

where μ_{t} is the turbulent viscosity defined according to the turbulence model.

Conservation of momentum is described:

$$\frac{\partial\left(\rho u_i c_p T\right)}{\partial x_j}=\frac{\partial}{\partial x_j}\left[\mu_{\text{eff}}\left(\frac{\partial u_i}{\partial x_j}+\frac{\partial u_j}{\partial x_i}\right)-\frac{2}{3}\mu_{\text{eff}}\frac{\partial u_k}{\partial x_k}\right]+\frac{\partial}{\partial \text{x}_{\text{i}}}\left(k_{\text{eff}}\frac{\partial T}{\partial x_i}\right) \tag{4}$$

where k_{eff} is the effective conductivity which is calculated:

$$k_{\text{eff}}=k+k_{\text{t}} \tag{5}$$

where k_{t} is the turbulent thermal conductivity defined according to the turbulence model.

The k-equation and ω-equation are described:

$$\frac{\partial(\rho u_j k)}{\partial x_j}=\frac{\partial}{\partial x_j}\left(\mu+\frac{\mu_t}{\sigma_k}\right)\frac{\partial k}{\partial x_j}+P_k-D_k+S_k \tag{6}$$

$$\frac{\partial(\rho u_j \omega)}{\partial x_j}=\frac{\partial}{\partial x_j}\left(\mu+\frac{\mu_{\text{t}}}{\sigma_\omega}\right)\frac{\partial \omega}{\partial x_j}+C_\omega+P_\omega-D_\omega+S_\omega \tag{7}$$

Data reduction

In the thermal system, high grade energy is partially converted into low grade energy due to irreversible factors such as the dissipation effect, and entropy generation is produced. The more irreversible factors and the greater the degree of irreversibility, the more entropy generation is produced. Irreversible factors are, to a certain extent, a manifestation of the degree of disorder in a system, so entropy generation is a large amount of disorder. The entropy generation is the product of the irreversibility of heat and friction. For any simulated pipe section j, the entropy generation ignoring thermal friction can be calculated [46]:

$$S_{g,j}=\frac{Q_j}{T_{w,j}}-\frac{Q_j}{T_{r,j}} \tag{8}$$

where $T_{w,i}$ and $T_{\text{r,j}}$ are the bulk temperature of water in section j and the bulk temperature of CO_2 in section j along the axial line, respectively, Q_j was heat exchange in section j which were calculated [47]:

$$Q_j=c_{p,w}\dot{m}_w\left(T_{w,\text{out},j}-T_{w,\text{in},j}\right) \tag{9}$$

where $c_{p,w}$ and $\dot{m}_w$ were the specific heat of water and mass-flow rate of water, respectively, $T_{w,\text{out},j}$ and $T_{w,\text{in},j}$ were the outlet and inlet temperature of water in section j.

When the system changes reversibly from any state to a state in equilibrium with the environment, the maximum amount that can theoretically be converted into useable work is called exergy. For a heat exchanger or a pipe section, the difference between input and recovery is the exergy destruction which was calculated:

$$E_k = \left(h_{r,\text{in},j} - h_{r,\text{out},j}\right) - T_0\left(S_{r,\text{in},j} - S_{r,\text{out},j}\right) \tag{10}$$

where $h_{r,\text{in},j}$ and $h_{r,\text{out},j}$ are the import and export enthalpy of CO_2 in section j, $S_{r,\text{in},j}$ and $S_{r,\text{out},j}$ – the import and export entropy of CO_2 in section j, T_0 – the ambient temperature, take a constant 298.15 K.

Entransy dissipation was calculated:

$$E_h = \int_0^T Q\text{d}T \tag{11}$$

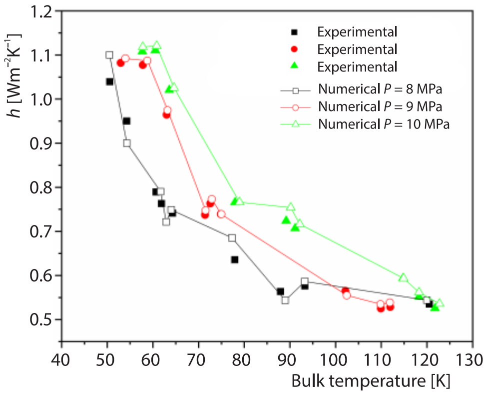

Figure 3. Comparison of numerical calculation results with experimental results

Reliability verification

Model validation

Since experiments on supercritical CO_2 double-pipe heat exchangers have been done previously, this paper directly used the previously obtained experimental data to verify the validity of the simulation. The specific equipment of the experiments and the working conditions can be found in [48]. Figure 3 showed a comparison of the numerical and experimental results for different pressures. The k-ω turbulent model is proved to be accurate and reliable in the heat transfer prediction.

Grid independence

Table 3 shows the pressure drop for different grid numbers. It can be seen that the pressure drop in the double pipe heat exchanger is no longer significant for a grid partition of $2.69 \cdot 10^6$. Therefore, a grid with the numbers $2.69 \cdot 10^6$ was selected to save computational time.

Table 3. Mesh independence verification

Number of meshes	Pressure drop	Error [%]
$1.28 \cdot 10^6$	1721.6	1.446845
$1.63 \cdot 10^6$	1283.1	0.823621
$1.86 \cdot 10^6$	1043.9	0.483655
$2.21 \cdot 10^6$	804.5	0.143405
$2.69 \cdot 10^6$	730	0.037521
$2.95 \cdot 10^6$	718.3	0.020893
$4.13 \cdot 10^6$	703.6	0

Results and discussions

Effects of CO_2 mass-flow rate

Figure 4 shows the distribution of entropy generation, exergy destruction, and entransy dissipation for different CO_2 flow rates in the y-axis direction. The CO_2 mass-flow rate changed from 0.19-0.58 kg/s, while cooling water mass-flow rate remained at 0.6 kg/s. In addition, the inlet temperature ($T_{r,\text{in}}$ = 343.15 K, $T_{w,\text{in}}$ = 299.15 K) is kept at a constant value. Both entropy generation and exergy destruction show a gradual decrease after CO_2 enters the heat exchanger tube in the radial direction (y-axis direction), and gradually decreases with increasing CO_2 mass-flow rate in the inlet pipe section from y = 0 m to y = 0.1 m as shown in figs. 4(a) and 4(b). The reason is that the pressure caused by the specific frictional resistance gradually decreases along the length of the tube, resulting in a decrease in the potential difference for irreversible losses, which leads to a gradual decrease in entropy generation, CO_2 is gradually cooled along the length of the tube, resulting in a gradual decrease in the amount of energy that can be converted into usable work, so that the exergy destruction gradually decreases at the same time. When the CO_2 mass-flow rate increases, the CO_2 bulk temperature decreases, and the heat transfer temperature difference between CO_2 and cooling water decreases, resulting in a lower imbalance potential and a lower entropy generation, while the energy that can be converted into useable work decreases with the lower CO_2 bulk temperature, so the exergy destruction also decreases. The high heat exchange in the inlet section leads to the high entransy dissipation at the inlet, and then the heat exchange decreases, and the fire entransy dissipation decreases gradually as can be seen in fig. 4(c). In fact, it can be seen from fig. 4 that the increase in CO_2 mass-flow rate has slight effect on the exergy destruction and entransy dissipation, after y = 0.1 m the entropy generation increases with increasing CO_2 mass-flow rate.

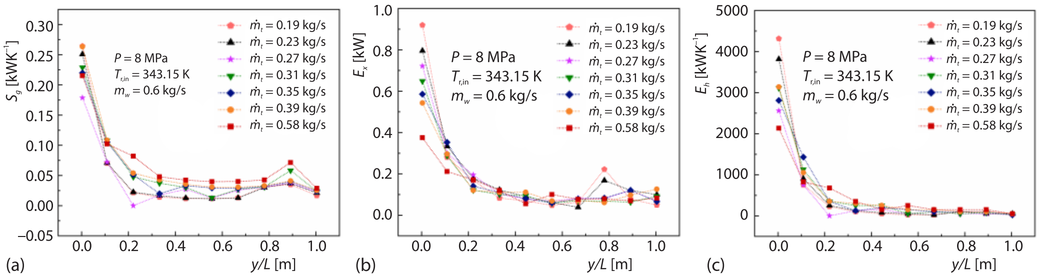

Figure 4. Effect of $\dot{m}_r$ on (a) entropy generation, (b) exergy destruction, and (c) entransy dissipation

Effects of water mass-flow rate

Figure 5 shows the distribution of entropy generation, exergy destruction, and entransy dissipation for different cooling water flow rates in the y-axis direction. Cooling water mass-flow rate changed from 0.6 kg/s to 1.2 kg/s, while the CO_2 mass-flow rate remained at 0.58 kg/s. The same inlet temperature ($T_{r,\text{in}}$ = 343.15 K, $T_{w,\text{in}}$ = 299.15 K) is kept at a constant value. The entropy generation, exergy destruction, and entransy dissipation all decrease gradually in the y-axis direction as can be seen in fig. 5, which is due to the gradual decrease of pressure along the tube length and the temperature drop of CO_2, and the gradual decrease of heat exchange in each section of the tube length, resulting in the decrease of unbalanced potential difference for irreversible losses, the decrease of energy that can be converted into usable work, and the decrease of *heat transfer capacity* losses. Entropy generation, exergy destruction, and entransy dissipation with the cooling water flow rate do not change significantly, which indicates that the increase in cooling water flow rate with the heat exchanger energy consumption is not significant, theoretically changing the mass-flow rate of cooling water on the heat exchanger design guidance is not significant.

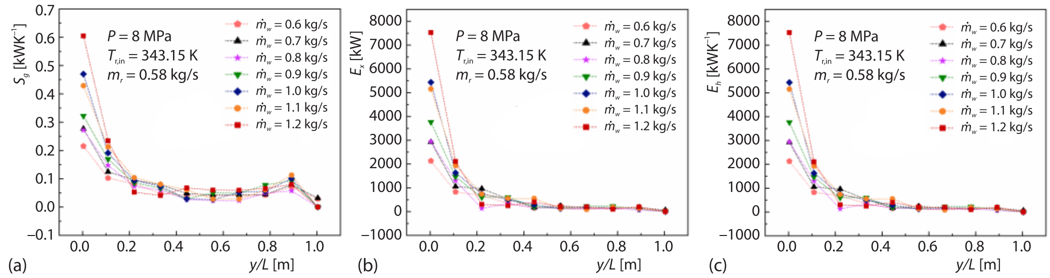

Figure 5. Effect of $\dot{m}_w$ on (a) entropy generation, (b) exergy destruction, and (c) entransy dissipation

Effects of pressure

Figure 6 shows the distribution of entropy generation, exergy destruction, and entransy dissipation for different pressure in the y-axis direction. The pressure changed from 7.5-12 MPa, CO_2 mass-flow rate remained at 0.58 kg/s and the cooling water mass-flow rate remained at 0.6 kg/s. The same inlet temperature ($T_{r,\mathrm{in}}$ = 343.15 K, $T_{w,\mathrm{in}}$ = 299.15 K) is kept at a constant value. the entropy generation, exergy destruction, and entransy dissipation decrease gradually along the y-axis at all pressures as shown in fig. 6. It is clear that the reduction of entropy generation and entransy dissipation at different pressures is significantly moderated when comparing different CO_2 and water flow rates. The entropy generation and entransy dissipation at y = 0 m to y = 0.05 m decrease with increasing pressure and the opposite after that. The higher the pressure, the greater the potential difference causing irreversible losses. The greater the potential difference of irreversible loss, so the more entropy generation, when the pressure on the high pressure side is larger, the greater the temperature slip on the high pressure side, more heat can be released, so the more heat that can be converted into usable work, so the exergy destruction increases. This phenomenon is largely related to the complex physical properties of CO_2 near the critical point, as the temperature of CO_2 changes, the sudden change in specific heat causes a change in heat exchange resulting in a sudden change in entropy generation and entransy dissipation. By comparing the seven pressure conditions, it is found that the higher the pressure, the higher the potential difference causing irreversible losses, so the higher entropy generation which is clearly shown in fig. 6(a). Changes in pressure have minimal effect on the exergy destruction.

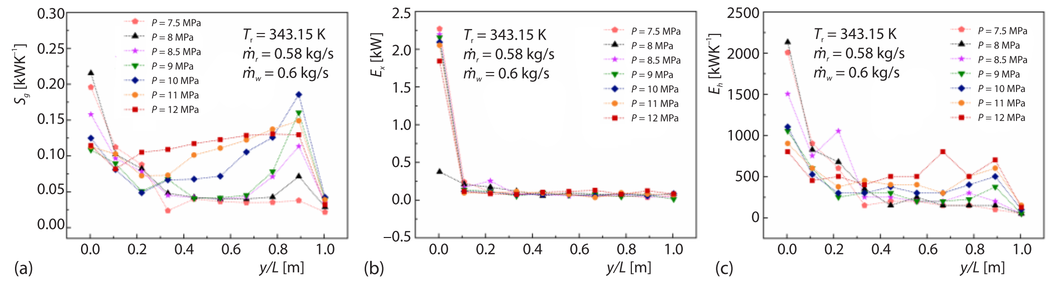

Figure 6. Effect of P on (a) entropy generation (b) exergy destruction, and (c) entransy dissipation

Effects of CO_2 inlet temperature

In order to clarify the effect of CO_2 inlet temperature on the energy efficiency of the heat exchanger, the CO_2 inlet temperature was varied from 343.15-388.15 K and the cold water temperature was kept at 299.15 K. Meanwhile, the mass-flow rates of cold water and CO_2 were kept at 0.6 kg/s and 0.58 kg/s, respectively. Figure 7 shows the distribution of entropy generation, exergy destruction, and entransy dissipation for different CO_2 inlet temperatures in the y-axis direction. It is obvious that the trend of the entropy generation, exergy destruction are the same as entransy dissipation, all decreasing along the y-axis direction, and the increase of the inlet temperature between $y = 0$ and $y = 0.5$ m leads to the increase of entropy generation, exergy destruction, and entransy dissipation but this situation disappears after $y = 0.5$ m. The high heat transfer temperature difference at the inlet is the reason for the existence of the aforementioned situation, and as the CO_2 temperature decreases and the cooling water temperature increases, the temperature difference between them decreases, which naturally makes this trend disappear.

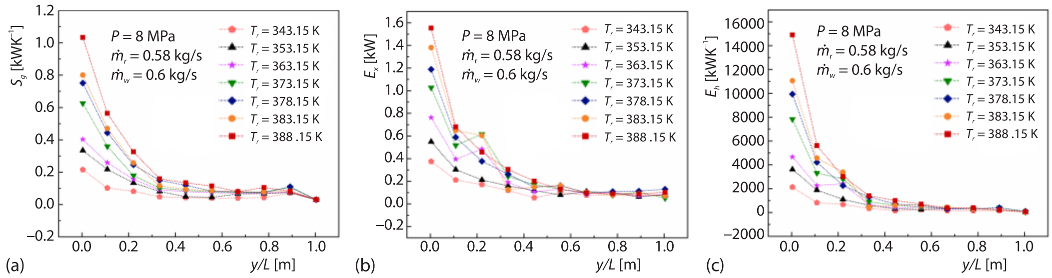

Figure 7. Effect of $T_{r,\mathrm{in}}$ on (a) entropy generation, (b) exergy destruction, and (c) entransy dissipation

Effects of water inlet temperature

To investigate the effect of water inlet temperature on the energy efficiency of the heat exchanger, the water inlet temperature was varied from 299.15-305.15 K and CO_2 inlet temperature was kept at 343.15 K. Meanwhile, the mass-flow rates of cold water and CO_2 were kept at 0.6 kg/s and 0.58 kg/s, respectively. Figure 8 shows the distribution of entropy generation, exergy destruction, and entransy dissipation for different water inlet temperatures in the y-axis direction. As shown in fig. 8, entropy generation, exergy destruction, and entransy dissipation show a strict decreasing trend along the y-axis direction. The entrance section is much higher than the other sections, in other words, the increase in temperature difference between the cold water inlet and the hot water inlet leads to an increase in entropy production.

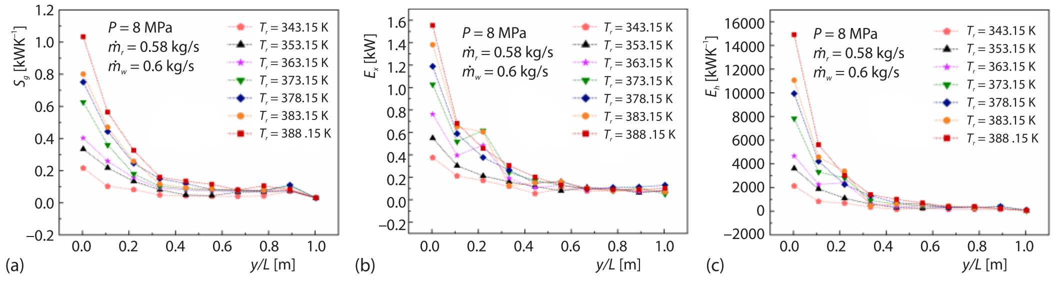

Figure 8. Effect of $T_{w,\mathrm{in}}$ on (a) entropy generation, (b) exergy destruction, and (c) entransy dissipation

Conclusions

In this study, numerical simulations based on the Second law of thermodynamics were performed on heat exchanger products that already exist in the market. The effects of CO_2 mass-flow rate, water mass-flow rate, pressure, CO_2 inlet temperature, and water inlet temperature on the heat transfer effectiveness of the heat exchanger were considered to evaluate the energy efficiency of the heat exchanger. The indexes entropy generation, exergy destruction, and entransy dissipation for evaluating the energy efficiency of heat exchangers are analyzed in detail in this paper. The following conclusions were drawn from this study.

The changes of the entropy generation, the changes of exergy destruction, and entransy dissipation are similar regardless of the operating conditions (CO_2 mass-flow rate, water mass-flow rate, pressure, CO_2 inlet temperature, and water inlet temperature), and the similarity is that they are decreasing in the direction of temperature decrease (y-axis direction).

Compared to other operating conditions, it is clear that pressure has the most significant effect on the energy efficiency of the heat exchanger. But the effect of pressure on the exergy destruction is negligible.

The effect of pressure on the energy efficiency of the heat exchanger differs before and after $y = 0.05$ m. The entropy generation and entransy dissipation at $y = 0$ m to $y = 0.05$ m decrease with increasing pressure and the opposite after that.

The effect of CO_2 inlet temperature on the energy efficiency of the heat exchanger differs before and after $y = 0.5$ m. The increase of the inlet temperature between $y = 0$ and $y = 0.5$ m leads to the increase of entropy generation, exergy destruction, and entransy dissipation but this situation disappears after $y = 0.5$ m.

Both entropy generation and exergy destruction show a gradual decrease after CO_2 enters the heat exchanger tube in the radial direction (y-axis direction), and gradually decreases with increasing CO_2 and water mass-flow rate in the inlet pipe section from $y = 0$ m to $y = 0.1$ m, but after that, the situation was completely opposite, entropy generation, exergy destruction, and CO_2 and water mass-flow rate are positively correlated.

Acknowledgment

This paper is supported by this research has been supported by Science and technology innovation action plan of Shanghai Science and Technology Commission (19DZ1207503) and the Shanghai Professional Technology Service Platform on Cold Chain Equipment Performance and Energy Saving Testing Evaluation (20DZ2292200).

References

[1] Hamed, S. D., *et al.*, A Comprehensive Second Law Analysis For Tube-in-Tube Helically Coiled Heat Exchangers, *Exp. Therm. Fluid Sci.*, *76* (2016), Sept., pp. 118-125

[2] Liu, X., *et al.*, Numerical Study of the Effect of Buoyancy Force and Centrifugal Force on Heat Transfer Characteristics of Supercritical CO_2 in Helically Coiled Tube At Various Inclination Angles, *Appl. Therm. Eng.*, *116* (2017), Apr., pp. 500-515

[3] Zhang, S., *et al.*, Experimental Investigation on the Heat Transfer Characteristics of Supercritical CO_2 at Various Mass-Flow Rates in Heated Vertical-Flow Tube, *Appl. Therm. Eng.*, *157* (2019), 113687

[4] Zhang, G.W., *et al.*, Experimental and Simulation Investigation on Heat Transfer Characteristics of In-Tube Supercritical CO_2 *Cooling Flow, Appl. Therm. Eng.*, *143* (2018), Oct., pp. 1101-1113

[5] Joneydi S. O., *et al.*, Comparison of Transcritical CO_2 Refrigeration Cycle with Expander and Throttling Valve Including/Excluding Internal Heat Exchanger: Exergy And Energy Points Of View, *Appl. Therm. Eng.*, *93* (2016), Jan., pp. 779-787

[6] Wang, Y., *et al.*, Energy, Exergy And Exergoeconomic Evaluation of the Air Source Transcritical CO_2 Heat Pump With Internal Heat Exchanger For Space Heating, *Int. J. Refrig.*, *130* (2021), Oct., pp. 14-26

[7] Elbarghthi, A. F. A., *et al.*, An Experimental Study of an Ejector-Boosted Transcritical R744 Refrigeration System Including An Exergy Analysis, *Energy Convers. Manag*., *238* (2021), 114102
[8] Zhang, H., *et al*., Heat Transfer Performance Of Supercritical Pressure CO_2 in A Non-Uniformly Heated Horizontal Tube, *Int. J. Heat Mass Transf*., *155* (2020), 119748
[9] Liu, X., *et al.*, Flow Structure with Mixed Turbulent Flow of Supercritical CO_2 Heated In Helically Coiled Tube, *Appl. Therm. Eng*., *189* (2021), 116684
[10] Yang, Z., *et al*., Effects of Longitudinal Vortex Generators on the Heat Transfer Deterioration of Supercritical CO_2 In Vertical Tubes, *Int. J. Heat Mass Transf.*, *152* (2020), 119478
[11] Sun, F., *et al*., An Artificial-Neural-Network Based Prediction of Heat Transfer Behaviors For in-Tube Supercritical CO_2 Flow, *Appl. Soft Comput.*, *102* (2021), 107110
[12] Luo, Z., *et al*., Prediction of Critical Heat Flux for Supercritical Water and CO_2 Flowing Upward in Vertical Heated Tubes, *Int. J. Heat Mass Transf.*, *159* (2020), 120115
[13] Yang, J., *et al.*, Improved Genetic Algorithm-Based Prediction of a CO_2 Micro-Channel Gas-Cooler Against Experimental Data In Automobile Air Conditioning System, *Int. J. Refrig.*, *106* (2019), Oct., pp. 517-525
[14] Li, J., *et al*., Experimental and Numerical Study of an Integrated Fin and Micro-Channel Gas Cooler for A CO_2 Automotive Air-Conditioning, *Appl. Therm. Eng*., *116* (2017), Apr., pp. 636-647
[15] Wang, D., *et al*., Heating Performance Evaluation of a CO_2 Heat Pump System for an Electrical Vehicle at Cold Ambient Temperatures, *Appl. Therm. Eng*., *142* (2018), July, pp. 656-664
[16] Cai, H. F., *et al.*, Numerical Investigation on Heat Transfer of Supercritical Carbon Dioxide in the Microtube Heat Exchanger at Low Reynolds Numbers, *Int. J. Heat Mass Transf*., *151* (2020), 119448
[17] Katz, A., *et al*., Experimental Investigation of Pressure Drop and Heat Transfer in High Temperature Supercritical CO_2 and Helium in A Printed-Circuit Heat Exchanger, *Int. J. Heat Mass Transf*., *171* (2021), 121089
[18] Bennett, K., Chen, Y. T., One-Way Coupled 3-D Fluid-Structure Interaction Analysis of Zigzag-Channel Supercritical CO_2 Printed Circuit Heat Exchangers, *Nucl. Eng. Des.*, *358* (2020), Oct., 110434
[19] Kim, S. G., *et al*., The CFD Aided Approach to Design Printed Circuit Heat Exchangers for Supercritical CO_2 Brayton Cycle Application, *Ann. Nucl. Energy*, *92* (2016), June, pp. 175-185
[20] Saeed, M., *et al*., Numerical Investigation of Thermal and Hydraulic Characteristics of SCO_2-Water Printed Circuit Heat Exchangers with Zigzag Channels, *Energy Convers. Manag*., *224* (2020), Aug., 113375
[21] Ameur, H., *et al*., Numerical Investigation of the Performance of Perforated Baffles in a Plate-Fin Heat Exchanger, *Thermal Science*, *25* (2021), 5B, pp. 3629-3641
[22] Menni, Y., *et al*., Improvement of the Performance of Solar Channels by Using Vortex Generators and Hydrogen Fluid, *Journal Therm. Anal. Calorim*., *147* (2020), Oct., pp. 545-566
[23] Karima, A., *et al*., The CFD Investigations of Thermal and Dynamic Behaviors in a Tubular Heat Exchanger With Butterfly Baffles, *Front. Heat Mass Transf*., *10* (2018), 27
[24] Han, Y., *et al.*, A Review of Development of Micro-Channel Heat Exchanger Applied in Air-Conditioning System, *Proceedings*, *Energy Procedia*, *14* (2012), Jan., pp. 148-153
[25] Jiang, P. X., *et al*., Experimental and Numerical Investigation of Convection Heat Transfer of CO_2 at Supercritical Pressures in a Vertical Tube at Low Reynolds Numbers, *Int. J. Therm. Sci.*, *47* (2008), 8, pp. 998-1011
[26] Jiang, P. X., *et al*., Convection Heat Transfer of CO_2 at Supercritical Pressures in a Vertical Mini Tube at Relatively Low Reynolds Numbers, *Exp. Therm. Fluid Sci*., *32* (2008), 8, pp. 1628-1637
[27] Jiang, P. X., *et al*., Experimental and Numerical Investigation of Convection Heat Transfer of CO_2 at Supercritical Pressures in a Vertical Mini-Tube, *Int. J. Heat Mass Transf*., *51* (2008), 11-12, pp. 3052-3056
[28] Xu, R. N., *et al*., Experimental Research on the Turbulent Convection Heat Transfer of Supercritical Pressure CO_2 in A Serpentine Vertical Mini Tube, *Int. J. Heat Mass Transf*., *91* (2015), Dec., pp. 552-561
[29] Zhang, Y., *et al.*, Numerical Investigation on Local Heat Transfer Characteristics of S-CO_2 in Horizontal Semicircular Microtube, *Appl. Therm. Eng*., *15*4 (2019), May, pp. 380-392
[30] Lei, X., *et al*., Experimental Study on Convection Heat Transfer of Supercritical CO_2 in Small Upward Channels, *Energy*, *176* (2019), June, pp. 119-130
[31] Cao, F., *et al*., Theoretical Analysis of Internal Heat Exchanger in Transcritical CO_2 Heat Pump Systems and Its Experimental Verification, *Int. J. Refrig*., *6* (2019), Oct., pp. 506-516
[32] Cao, F., *et al*., Experimental Investigation on the Influence of Internal Heat Exchanger in a Transcritical CO_2 Heat Pump Water Heater, *Appl. Therm. Eng*., *168* (2020), 114855
[33] Fang, J., *et al*., Cooling Performance Enhancement for the Automobile Transcritical CO_2 Air Conditioning System with Various Internal Heat Exchanger Effectiveness, *Appl. Therm. Eng*., *196* (2021), 117274

[34] Hashemian, M., *et al*., A Comprehensive Numerical Study on Multi-Criteria Design Analyses in a Novel Form (Conical) of Double Pipe Heat Exchanger, *Appl. Therm. Eng*., *102* (2016), June, pp. 1228-1237
[35] Jafarzad, A., Heyhat, M. M., Thermal and Exergy Analysis of Air- Nanofluid Bubbly Flow in a Double-Pipe Heat Exchanger, *Powder Technol*., *372* (2020), July, pp. 563-577
[36] Chen, W., *et al*., Numerical Investigation of Heat Transfer and Flow Characteristics of Supercritical CO_2 in U-Duct, *Appl. Therm. Eng*., *144* (2018), Nov., pp. 532-539
[37] Yang, Z., *et al.*, Numerical Study on the Heat Transfer Enhancement of Supercritical CO_2 in Vertical Ribbed Tubes, *Appl. Therm. Eng*., *145* (2018), Dec., pp. 705-715
[38] Zhang, S., *et al*., Experimental and Numerical Comparison of the Heat Transfer Behaviors and Buoyancy Effects of Supercritical CO_2 in Various Heating Tubes, *Int. J. Heat Mass Transf*., *149* (2020), Mar., 119074
[39] Wang, H., Kissick, S. M., Modelling and Simulation of a Supercritical CO_2-Liquid Sodium Compact Heat Exchanger for Sodium-Cooled Fast Reactors, *Appl. Therm. Eng*., *180* (2020), 115859
[40] Aly, W. I. A., Numerical Study on Turbulent Heat Transfer And Pressure Drop of Nanofluid in Coiled Tube-in-Tube Heat Exchangers, *Energy Convers. Manag*., *79* (2014), Mar., pp. 304-316
[41] Sadighi Dizaji, H., *et al*., Experimental Studies on Heat Transfer and Pressure Drop Characteristics for new Arrangements of Corrugated Tubes in a Double Pipe Heat Exchanger, *Int. J. Therm. Sci*., *96* (2015), Oct., pp. 211-220
[42] Sadighi Dizaji, H., *et al.*, The Effect of Flow, Thermodynamic and Geometrical Characteristics on Exergy Loss in Shell and Coiled Tube Heat Exchangers, *Energ*y, *91* (2015), Nov., pp. 678-684
[43] Safikhani, H., Eiamsa-Ard, S., Pareto Based Multi-Objective Optimization of Turbulent Heat Transfer Flow in Helically Corrugated Tubes, *Appl. Therm. Eng*., *95* (2016), Feb., pp. 275-280
[44] El Maakoul, A., *et al.*, Numerical Investigation of Thermohydraulic Performance of Air to Water Double-Pipe Heat Exchanger With Helical Fins, *Appl. Therm. Eng.*, *127* (2017), Dec., pp. 127-139
[45] Ali, S.K., *et al.*, Experimental Validation and Numerical Investigation for Optimization and Evaluation of Heat Transfer Enhancement in Double Coil Heat Exchanger, *Therm. Sci. Eng. Prog.*, *22* (2021), 100862
[46] Manjunath, K., Kaushik, S. C., Second Law Thermodynamic Study of Heat Exchangers: A Review, *Renew. Sustain. Energy Rev*., *40* (2014), Dec., pp. 348-374
[47] Joppolo, C. M., *et al*., Numerical Analysis of the Influence of Circuit Arrangement on a Fin-and-Tube Condenser Performance, *Case Stud. Therm. Eng*., *6* (2015), Sept., pp. 136-146
[48] Yang, D., *et al*., An Experimental and Numerical Study of Helix Tube Gas Cooler for Super-Critical Carbon Dioxide, *Journal Chem. Eng. Japan*, *50* (2017), 12, pp. 900-908

Paper submitted: July 19, 2021
Paper revised: October 15, 2021
Paper accepted: November 4, 2021